A&A 573, A31 (2015)
DOI: 10.1051/0004-6361/201321436

Astronomy & Astrophysics

The high-energy γ-ray emission of AP Librae *(Research Note)*

H.E.S.S. Collaboration, A. Abramowski[1], F. Aharonian[2,3,4], F. Ait Benkhali[2], A. G. Akhperjanian[5,4], E. Angüner[6], G. Anton[7], M. Backes[8], S. Balenderan[9], A. Balzer[10,11], A. Barnacka[12], Y. Becherini[13], J. Becker Tjus[14], K. Bernlöhr[2,6], E. Birsin[6], E. Bissaldi[15], J. Biteau[16,17,⋆], M. Böttcher[18], C. Boisson[19], J. Bolmont[20], P. Bordas[21], J. Brucker[7], F. Brun[2], P. Brun[22], T. Bulik[23], S. Carrigan[2], S. Casanova[18,2], P. M. Chadwick[9], R. Chalme-Calvet[20], R. C. G. Chaves[22], A. Cheesebrough[9], M. Chrétien[20], S. Colafrancesco[24], G. Cologna[25], J. Conrad[26,27], C. Couturier[20], Y. Cui[21], M. Dalton[28,29], M. K. Daniel[9], I. D. Davids[18,8], B. Degrange[16], C. Deil[2], P. deWilt[30], H. J. Dickinson[26], A. Djannati-Ataï[31], W. Domainko[2], L. O'C. Drury[3], G. Dubus[32], K. Dutson[33], J. Dyks[12], M. Dyrda[34], T. Edwards[2], K. Egberts[15], P. Eger[2], P. Espigat[31], C. Farnier[26], S. Fegan[16], F. Feinstein[35], M. V. Fernandes[1], D. Fernandez[35], A. Fiasson[36], G. Fontaine[16], A. Förster[2], M. Füßling[11], M. Gajdus[6], Y. A. Gallant[35], T. Garrigoux[20], G. Giavitto[10], B. Giebels[16], J. F. Glicenstein[22], M.-H. Grondin[2,25], M. Grudzińska[23], S. Häffner[7], J. Hahn[2], J. Harris[9], G. Heinzelmann[1], G. Henri[32], G. Hermann[2], O. Hervet[19], A. Hillert[2], J. A. Hinton[33], W. Hofmann[2], P. Hofverberg[2], M. Holler[11], D. Horns[1], A. Jacholkowska[20], C. Jahn[7], M. Jamrozy[37], M. Janiak[12], F. Jankowsky[25], I. Jung[7], M. A. Kastendieck[1], K. Katarzyński[38], U. Katz[7], S. Kaufmann[25], B. Khélifi[31], M. Kieffer[20], S. Klepser[10], D. Klochkov[21], W. Kluźniak[12], T. Kneiske[1], D. Kolitzus[15], Nu. Komin[36], K. Kosack[22], S. Krakau[14], F. Krayzel[36], P. P. Krüger[18,2], H. Laffon[28], G. Lamanna[36], J. Lefaucheur[31], A. Lemière[31], M. Lemoine-Goumard[28], J.-P. Lenain[20], T. Lohse[6], A. Lopatin[7], C.-C. Lu[2], V. Marandon[2], A. Marcowith[35], R. Marx[2], G. Maurin[36], N. Maxted[30], M. Mayer[11], T. J. L. McComb[9], J. Méhault[28,29], P. J. Meintjes[39], U. Menzler[14], M. Meyer[26], R. Moderski[12], M. Mohamed[25], E. Moulin[22], T. Murach[6], C. L. Naumann[20], M. de Naurois[16], J. Niemiec[34], S. J. Nolan[9], L. Oakes[6], H. Odaka[2], S. Ohm[33], E. de Oña Wilhelmi[2], B. Opitz[1], M. Ostrowski[37], I. Oya[6], M. Panter[2], R. D. Parsons[2], M. Paz Arribas[6], N. W. Pekeur[18], G. Pelletier[32], J. Perez[15], P.-O. Petrucci[32], B. Peyaud[22], S. Pita[31], H. Poon[2], G. Pühlhofer[21], M. Punch[31], A. Quirrenbach[25], S. Raab[7], M. Raue[1], I. Reichardt[31], A. Reimer[15], O. Reimer[15], M. Renaud[35], R. de los Reyes[2], F. Rieger[2], L. Rob[40], C. Romoli[3], S. Rosier-Lees[36], G. Rowell[30], B. Rudak[12], C. B. Rulten[19], V. Sahakian[5,4], D. A. Sanchez[36], A. Santangelo[21], R. Schlickeiser[14], F. Schüssler[22], A. Schulz[10], U. Schwanke[6], S. Schwarzburg[21], S. Schwemmer[25], H. Sol[19], G. Spengler[6], F. Spies[1], Ł. Stawarz[37], R. Steenkamp[8], C. Stegmann[11,10], F. Stinzing[7], K. Stycz[10], I. Sushch[6,18], J.-P. Tavernet[20], T. Tavernier[31], A. M. Taylor[3], R. Terrier[31], M. Tluczykont[1], C. Trichard[36], K. Valerius[7], C. van Eldik[7], B. van Soelen[39], G. Vasileiadis[35], C. Venter[18], A. Viana[2], P. Vincent[20], H. J. Völk[2], F. Volpe[2], M. Vorster[18], T. Vuillaume[32], S. J. Wagner[25], P. Wagner[6], R. M. Wagner[26], M. Ward[9], M. Weidinger[14], Q. Weitzel[2], R. White[33], A. Wierzcholska[37], P. Willmann[7], A. Wörnlein[7], D. Wouters[22], R. Yang[2], V. Zabalza[2,33], M. Zacharias[25], A. A. Zdziarski[12], A. Zech[19], H.-S. Zechlin[1], J. Finke[41], P. Fortin[42], and D. Horan[16]

(Affiliations can be found after the references)

Received 8 March 2013 / Accepted 20 October 2014

ABSTRACT

The γ-ray spectrum of the low-frequency-peaked BL Lac (LBL) object AP Librae is studied, following the discovery of very-high-energy (VHE; $E > 100$ GeV) γ-ray emission up to the TeV range by the H.E.S.S. experiment. This makes AP Librae one of the few VHE emitters of the LBL type. The measured spectrum yields a flux of $(8.8 \pm 1.5_{\rm stat} \pm 1.8_{\rm sys}) \times 10^{-12}$ cm^{-2} s^{-1} above 130 GeV and a spectral index of $\Gamma = 2.65 \pm 0.19_{\rm stat} \pm 0.20_{\rm sys}$. This study also makes use of *Fermi*-LAT observations in the high energy (HE, $E > 100$ MeV) range, providing the longest continuous light curve (5 years) ever published on this source. The source underwent a flaring event between MJD 56 306–56 376 in the HE range, with a flux increase of a factor of 3.5 in the 14 day bin light curve and no significant variation in spectral shape with respect to the low-flux state. While the H.E.S.S. and (low state) *Fermi*-LAT fluxes are in good agreement where they overlap, a spectral curvature between the steep VHE spectrum and the *Fermi*-LAT spectrum is observed. The maximum of the γ-ray emission in the spectral energy distribution is located below the GeV energy range.

Key words. galaxies: active – BL Lacertae objects: individual: AP Librae – gamma rays: galaxies

1. Introduction

The BL Lac class of blazars constitutes about 45% of both the First (Abdo et al. 2010b; 1LAC) and Second (Ackermann et al. 2011; 2LAC) *Fermi* Large Area Telescope (LAT) Catalogue of active galactic nuclei (AGN), and constitutes the majority of

⋆ Corresponding authors:
David Sanchez, e-mail: david.sanchez@lapp.in2p3.fr;
Pascal Fortin, e-mail: pafortin@cfa.harvard.edu;
Jonathan Biteau, e-mail: biteau@in2p3.fr

the extragalactic very-high-energy (VHE, $E > 100$ GeV) γ-ray sources[1]. AP Librae falls into the category of low-frequency-peaked BL Lac (LBL), defined by an X-ray to radio flux ratio of $f_x/f_r < 10^{-11}$ (Padovani & Giommi 1995), and of the more recently introduced low frequency synchrotron peaked (LSP) class of blazars defined by a synchrotron emission peak in the spectral energy distribution (SED) at $\nu_{s,\,peak} \leq 10^{14}$ Hz (see Abdo et al. 2010c,d). This is an order of magnitude lower than the $\nu_{s,\,peak}$ values found in the bulk of VHE γ-ray emitting blazars, which belong to the high-frequency-peaked BL Lac/high frequency synchrotron peaked (HBL/HSP) class. A continuity between these classes of blazars is suggested by the blazar sequence (Fossati et al. 1998), where the dominance of the high-energy component and its peak emission energy are inversely proportional to the total luminosity.

AP Librae was among the first objects to be classified as a member of the BL Lac class (Strittmatter et al. 1972), for which a reliable redshift could be measured ($z = 0.049 \pm 0.002$; Disney et al. 1974). The initial redshift measurement is consistent with the most recent measurement from the 6dF galaxy survey ($z = 0.0490 \pm 0.0001$; Jones et al. 2009). An object coincident with AP Librae was discovered in the radio band (PKS 1514–24) during a survey made with the 210 ft reflector at Parkes (Bolton et al. 1964), but it was not until 1971 that the optically variable source AP Librae and the radio source PKS 1514–24 were formally associated (Bond 1971; Biraud 1971). The host galaxy harbors a black hole at its center with a mass, estimated using stellar velocity dispersion, of $10^{8.40\pm0.06}\ M_\odot$ (Woo et al. 2005).

In X-rays, AP Librae was first detected by the *Einstein* X-Ray Observatory (1E 1514.7−2411; Schwartz & Ku 1983). At high energies (HE, $E > 100$ MeV), the source 3EG J1517−2538 (Hartman et al. 1999) was tentatively associated with AP Librae. The photon index reported in the third EGRET catalogue was rather soft ($\Gamma_{HE} = 2.66 \pm 0.43$), resulting in a low extrapolated flux level in the VHE range covered by atmospheric Cherenkov telescopes. Observations with the University of Durham Mark 6 γ-ray telescope resulted in a flux upper limit of 3.7×10^{-11} cm^{-2} s^{-1} for $E > 300$ GeV (Armstrong et al. 1999; Chadwick et al. 1999).

An early catalogue of bright γ-ray sources detected by the *Fermi*-LAT was produced using the first three months of data (Abdo et al. 2009a). One of these sources, 0FGL J1517.9−2423, was associated with AP Librae, but its photon index was harder ($\Gamma_{HE} = 1.94 \pm 0.14$, Abdo et al. 2009b) than that reported for 3EG J1517−2538. The extrapolation of its spectrum to higher energies raised the possibility of a detection by Cherenkov telescopes. In 2010, the H.E.S.S. Collaboration reported the detection of VHE γ rays from AP Librae (Hofmann 2010). Following this announcement, Fortin et al. (2010) showed the first radio-to-TeV SED, based on the preliminary analysis of an HE–VHE data set included in the larger one presented here, while Kaufmann et al. (2011) also pointed out the existence of an X-ray jet resolved with *Chandra*, making Ap Librae the only known TeV BL Lac object with an extended jet in X-rays.

The paper is organized as follows: in Sect. 2.1, H.E.S.S. observations are presented while the data analysis of five years of *Fermi*-LAT data is discussed in Sect. 2.2. The variability and broadband γ-ray emission of AP Librae are discussed in Sect. 3.

[1] An up-to-date VHE γ-ray catalogue can be found in the TeVCat, http://tevcat.uchicago.edu

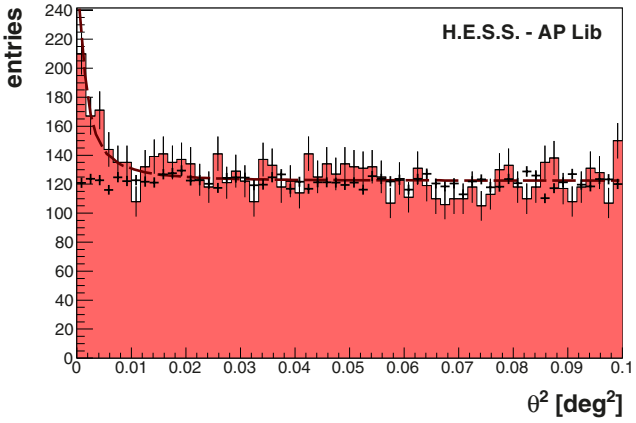

Fig. 1. Number of on-source candidate γ-ray events (solid histogram) and normalized off-source events (crosses), as a function of the squared angular distance θ^2 from the position of AP Librae, compared to a fit of a modeled PSF (dashed line).

2. Observations

2.1. H.E.S.S. observations

The High Energy Stereoscopic System (H.E.S.S.), located in the Khomas Highland in Namibia (23°16′18″ S, 16°30′01″ E), is an array of telescopes (four at the time of the observations studied) that detect the Cherenkov light flashes from air showers. H.E.S.S. observed AP Librae between MJD 55 326 (10 May 2010) and MJD 55 689 (8 May 2011) for a total of 34 observations of 28 min, each passing data-quality selection criteria (described in Aharonian et al. 2006). This yields an exposure of 14 h acceptance-corrected live time with a mean zenith angle of 13°. In order to minimize the spectral gap between *Fermi*-LAT and H.E.S.S., cuts achieving the lowest possible energy threshold were selected. The *loose cuts* (Aharonian et al. 2006), which require a minimum shower image intensity of 40 photoelectrons in each camera, were applied to the data set to perform the event selection, yielding an average energy threshold of $E_{th} = 130$ GeV. The model analysis method (de Naurois & Rolland 2009) was used to analyze the data within a 0.11° radius disk centered on the radio core position of AP Librae ($\alpha_{J2000} = 15^h\,17^m\,41.76^s$, $\delta_{J2000} = -24°\,22'\,19.6''$, Johnston et al. 1995) and further extract the spectrum and light curve, using the reflected-region method (Berge et al. 2007) to estimate the background contamination. With 1133 on-source events, 9042 off-source events and an on-off normalization of $\alpha = 0.10$, the significance of the 218 γ rays excess is 6.6σ (standard deviations, Li & Ma 1983). In Fig. 1, the background (black crosses) and on-source events distributions (solid histogram) are shown as a function of the squared angular distance between the source position and the γ-ray direction. The H.E.S.S. point-spread function (PSF) was fitted to the on-source events and matches well both the signal and the background for large angular distances.

A point-like source model, convolved with the PSF, has been fitted to the data. The position obtained through this fit is $\alpha_{J2000} = 15^h17^m40.6^s \pm 3.0^s_{stat} \pm 1.3^s_{sys}$ and $\delta_{J2000} = -24°\,22'\,37.5'' \pm 18.4''_{stat} \pm 20''_{sys}$, compatible within the statistical errors with the location of the AP Librae core 24″ away (Johnston et al. 1995). Further morphological studies confirm the absence of source extension within the H.E.S.S. PSF.

The time-averaged photon spectrum for these data is shown in Fig. 2. The best fit is a power-law function, within the energy

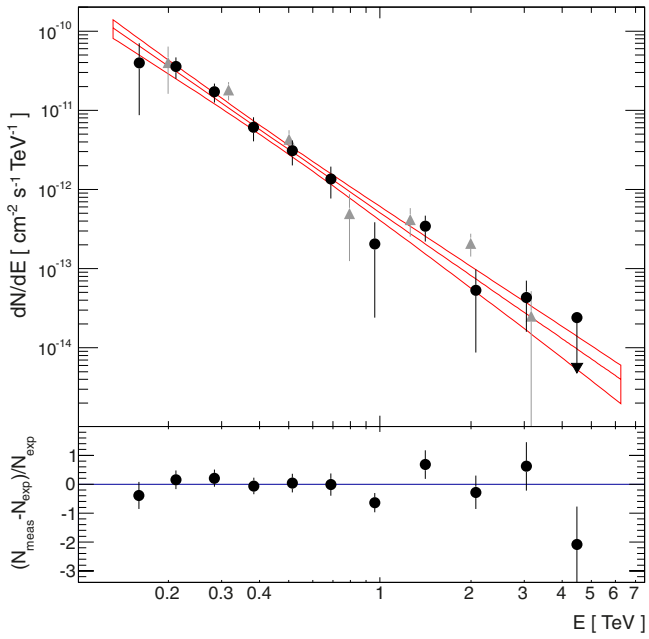

Fig. 2. Differential VHE γ-ray spectrum and corresponding butterfly of AP Librae as derived with the *Model* analysis. Uncertainties on the spectral points are given at 1σ, i.e., at the 68.3% confidence level, and upper limits are computed at the 99% confidence level. The residuals, which are the difference between the measured and expected number of γ rays in a bin divided by the expected number of γ rays, are shown in the lower panel. The light gray points in the upper plot represent the spectrum derived as a cross-check with the *Hillas* analysis. Errors are statistical only.

range 130 GeV−6.3 TeV, with a χ^2 probability of $P(\chi^2) = 40\%$, given by

$$\frac{\mathrm{d}N}{\mathrm{d}E} = (4.30 \pm 0.57_{\mathrm{stat}} \pm 0.86_{\mathrm{sys}}) \times 10^{-12} \times \left(\frac{E}{E_{\mathrm{dec}}}\right)^{-2.65 \pm 0.19_{\mathrm{stat}} \pm 0.20_{\mathrm{sys}}} \mathrm{cm}^{-2}\,\mathrm{s}^{-1}\,\mathrm{TeV}^{-1}, \quad (1)$$

where $E_{\mathrm{dec}} = 450$ GeV is the decorrelation energy. The best-fit parameters are obtained using a forward folding technique (Piron et al. 2001). Spectral points are derived with a similar approach in restricted energy ranges, with a fixed (to the best fit value) power-law index and a free normalization.

This result was cross-checked with a standard *Hillas* analysis (Aharonian et al. 2006) with the *loose cuts*, based also on a different calibration chain. It was found to be entirely compatible with the *Model* analysis and yielding a detection significance of 6.7σ and a photon index of $\Gamma_{\mathrm{VHE}} = 2.63 \pm 0.25$ (see also the comparison of both spectra in Fig. 2). The upper limit on the flux derived from observations taken with the University of Durham Mark 6 γ-ray telescope (Chadwick et al. 1999), corresponding to ∼30% of the Crab Nebula flux at $E > 300$ GeV, is also compatible with the H.E.S.S. spectrum since it is well above the flux level measured here.

The light curve of the integral flux above 130 GeV, averaged over the time between two successive full moons, is shown in Fig. 3. A constant function fit to the time series yields a $P(\chi^2) = 36\%$ (χ^2/ndf = 3.2/3), which indicates that the light curve does not show any significant variability within the observed statistical errors. A 99% confidence level upper limit on the fractional variance (as defined in Vaughan et al. 2003) of

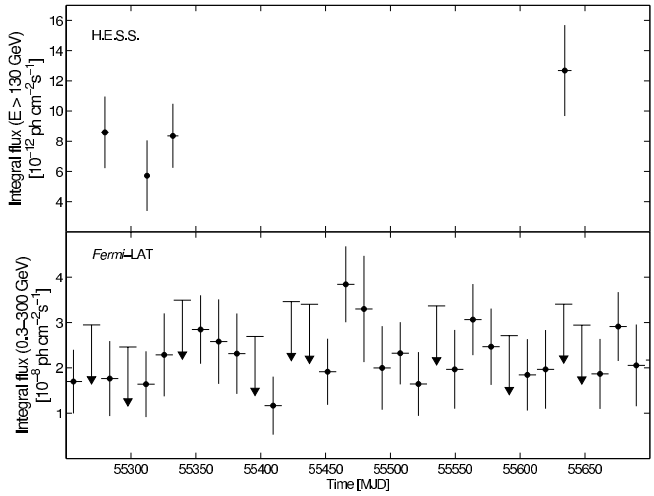

Fig. 3. Light curves derived from the observations described in Sect. 2 from MJD 55 250 to MJD 55 700 (corresponding to the H.E.S.S. measurements). The top panel presents the H.E.S.S. integral flux for $E > 130$ GeV where the horizontal bars represent the observing duration elapsed between the two successive full moon periods when H.E.S.S. observed the target. The *bottom panel* gives the *Fermi*-LAT 300 MeV–300 GeV flux, with 95% confidence level upper limits for segments where TS < 10 and the horizontal bars show the 14 day *Fermi*-LAT integration times. This sample is typical from what was seen throughout the quiescent state.

$F_{\mathrm{var}} < 0.46$ is derived (Feldman & Cousins 1998). No variability is found using the *Hillas* analysis with the different calibration.

2.2. Fermi-LAT observations

The *Fermi*-LAT, launched on 2008 June 11, is a pair-conversion γ-ray detector sensitive to photons in the energy range from 20 MeV to more than 300 GeV (Atwood et al. 2009). The data for this analysis were taken from 4 August 2008 to 4 August 2013 (MJD 54 682–56 508, 5 years) and were analyzed using the standard *Fermi* analysis software (ScienceTools v9r32p4) available from the *Fermi* Science Support Center (FSSC)[2]. Events with energy between 300 MeV and 300 GeV were selected from the Pass 7 data set. Only events passing the SOURCE class filter and located within a square region of side length 20° centered on AP Librae were selected. Cuts on the zenith angle (<100°) and rocking angle (<52°) were also applied to the data. The post-launch `P7SOURCE_V6` instrument response functions (IRFs) were used in combination with the corresponding Galactic and isotropic diffuse emission models[3]. The model of the region includes the diffuse components and all sources from the Second *Fermi*-LAT Catalog (2FGL, Nolan et al. 2012) located within a square region of side 24° centered on AP Librae. The spectral parameters of the sources were left free during the fitting procedure. A power-law correction in energy with free normalization and spectral slope was applied to the Galactic diffuse component. Events were analyzed using the binned maximum likelihood method as implemented in `gtlike`.

The source underwent a flaring episode of approximately 10 weeks between MJD 56 306–56 376 (flaring state). We have therefore defined a quiescent state measured during the periods MJD 54 682–56 305 and MJD 56 377–56 508.

[2] http://fermi.gsfc.nasa.gov/ssc/
[3] http://fermi.gsfc.nasa.gov/ssc/data/access/lat/BackgroundModels.html

AP Librae is detected with a high test statistic of TS = 2037 ($\approx 45\sigma$, Mattox et al. 1996) in the quiescent state. The energy spectrum evaluated using this data set is well described by a power-law with a photon index $\Gamma_{\rm HE} = 2.11 \pm 0.03_{\rm stat} \pm 0.05_{\rm sys}$, in good agreement with the 2FGL value, with no significant indication for spectral curvature. The 300 MeV–300 GeV integral flux is $F_{0.3-300\,\rm GeV} = (2.04 \pm 0.08_{\rm stat}{}^{+0.13}_{-0.12\rm sys}) \times 10^{-8}\,\rm cm^{-2}\,s^{-1}$, and the most energetic photon within the 95% containment radius of the *Fermi*-LAT PSF has an energy of 71 GeV. The systematic uncertainties were evaluated using the bracketing IRFs technique (Ackermann et al. 2012).

Replacing the power-law with a log-parabola[4] only results in a marginal improvement in likelihood ($2\Delta\log L = 10.3$ for 1 degree of freedom, or approximately 3.1σ). With this model, the best fit differential flux is $N_0 = (1.76 \pm 0.10) \times 10^{-13}\,\rm ph\,MeV^{-1}\,cm^{-2}\,s^{-1}$ at $E_0 = 5.48$ GeV with an index $\alpha = 2.21 \pm 0.06$ and a curvature parameter $\beta = 0.07 \pm 0.02$.

The *Fermi*-LAT 1σ spectral error contour for the power-law model of AP Librae is presented in Fig. 4. Flux values for individual energy bins were calculated independently, assuming a power-law spectral shape. For each energy bin, the spectral indices of all sources modeled in the region of interest were frozen to the best-fit values obtained for the full energy range and `gtlike` was used to determine the flux. The superimposed vertical error bars show the statistical uncertainties and the quadratic sum of statistical and systematic uncertainties, respectively. The latter were estimated by Ackermann et al. (2012) to be 10% of the effective area at 100 MeV, 5% at 560 MeV and 10% at 10 GeV and above. 95% confidence level upper limits were calculated for energy bins with TS values below 10. For completeness, the result of the log-parabola fit is also shown in Fig. 4.

The variability analysis of the LAT data showed a significant flare starting in 2013 January. During the flaring period MJD 56 306–56 376, the spectrum is well fitted by a power law with a total flux $F_{0.3-300\,\rm GeV} = (5.55 \pm 0.57_{\rm stat}{}^{+0.36}_{-0.32\rm sys}) \times 10^{-8}\,\rm cm^{-2}\,s^{-1}$ and a spectral index $\Gamma_{\rm HE} = 2.11 \pm 0.09_{\rm stat} \pm 0.05_{\rm sys}$, consistent in shape with the spectrum during the quiescent period (see Fig. 4). The peak flux in the two-week bin light curve is $(7.0 \pm 1.0) \times 10^{-8}\,\rm cm^{-2}\,s^{-1}$. The flaring state is discussed more extensively in Sect. 3.1. During this period, some observations were performed with the H.E.S.S. array, but the resulting data were too limited to be useful[5].

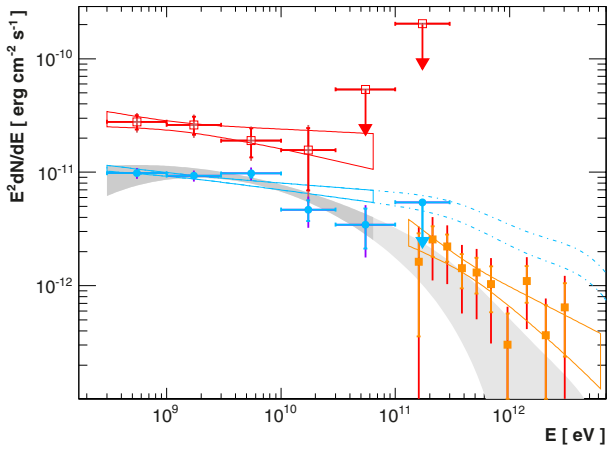

Fig. 4. γ-ray SED of AP Librae from *Fermi*-LAT (blue circles) and H.E.S.S. (orange squares and butterfly power-law fit). For the quiescent state, the *Fermi*-LAT best-fit power-law (blue butterfly) has been extrapolated toward the H.E.S.S. energy range taking EBL absorption into account (dash-dotted line). The *Fermi*-LAT log-parabola fit is shown in gray, and its extrapolation taking the EBL absorption into account is shown in light gray. The flare SED as measured by *Fermi*-LAT is given by the red butterfly and open squares. The shorter and longer errors bars indicate statistical-only and the quadratic sum of statistical and systematic uncertainties, respectively (see text).

3. Discussion

3.1. The flaring state of AP Librae

The *Fermi*-LAT light curve of the flaring episode above 300 MeV is shown in Fig. 5. The peak flux was 3.5 times greater than the averaged flux. The fastest doubling timescale (as defined in Zhang et al. 1999), corresponds to the rising part and has a value of 19 ± 11 days. The lightcurve has also been fitted with an asymmetric profile[6] $\phi(t) = A\exp(-|t - t_{\rm max}|/\sigma_{\rm r,d}) + B$ where the time of the peak is $t_{\rm max}$ and the rise and decay time are $\sigma_{\rm r}$ and $\sigma_{\rm d}$. B is a constant that is also fitted to the data. Fitting this function to the data yields a peak at $t_{\rm max}$(MJD) = 56 315.1 ± 2.7, of amplitude $A = (5.4 \pm 1.4) \times 10^{-8}\,\rm cm^{-2}\,s^{-1}$, above a constant value of $B = (2.4 \pm 0.6) \times 10^{-8}\,\rm cm^{-2}\,s^{-1}$ compatible with the low-state flux, for a $\chi^2/\rm d.o.f. = 6.7/7$. The rise time and decay time are found to be $\sigma_{\rm r} = 5.9 \pm 5.1$ days and $\sigma_{\rm d} = 27 \pm 12$ days, respectively. The rise time (or the doubling timescale) is compatible with 0 at a 2σ level, indicating a fast process but the lack of statistics prevents a more precise probe of this event by making shorter time bins. Substructures of the flare possibly present on shorter timescale might be hidden (see Saito et al. 2013, in which study complex flare structures were found when probing smaller timescale). An asymmetry in the rise and decay has already been seen in the GeV range for PKS 1502+106 (Abdo et al. 2010a) and in the TeV range during the 2006 flare of PKS 2155−304 (Aharonian et al. 2007). The opposite behavior, i.e., a smaller decay timescale, has nevertheless been observed in the TeV range in the radio galaxy M 87 (Abramowski et al. 2012). However the timescale of the event reported in this work is much longer and might be of a different origin (e.g., the onset and decay of large scale structural changes in the jet or possibly a change in accretion parameters).

3.2. The LBL AP Librae

The first evidence of VHE γ rays from an LBL-class blazar was the detection of BL Lacertae ($z = 0.069$) at the 5.1σ significance level (Albert et al. 2007) corresponding to a flux 3% that of the Crab Nebula. Its steep VHE spectrum ($\Gamma_{\rm VHE} = 3.6 \pm 0.5$) did not connect smoothly with the harder *Fermi*-LAT spectrum (Abdo et al. 2009c; $\Gamma_{\rm HE} = 2.43 \pm 0.10$) established after the measurement in VHE, but given the significant variability of the HE γ-ray flux of BL Lacertae (see Sokolovsky et al. 2010; Cutini 2011, 2012 and follow-up ATels), it is possible that the source was in a high VHE flux state at the time it was detected. Further evidence of VHE γ-ray emission from LBL-type objects was found with the detection of S5 0716+714 (Anderhub et al. 2009), a source with a steep VHE spectrum ($\Gamma_{\rm VHE} = 3.5 \pm 0.5$) and a harder HE spectrum (Ackermann et al. 2011; $\Gamma_{\rm HE} = 2.00 \pm 0.02$). It appears that AP Librae

[4] The log-parabola model is defined as $\mathrm{d}N/\mathrm{d}E = N_0 \left(\frac{E}{E_0}\right)^{-(\alpha+\beta\log(E/E_0))}$

[5] Less than 1 h of useful time was recorded during the flare. The limited duration and poor background estimation do not even give a useful limit on the flux.

[6] A symmetric Gaussian profile is rejected at a level of 20σ with respect to the function used in this work.

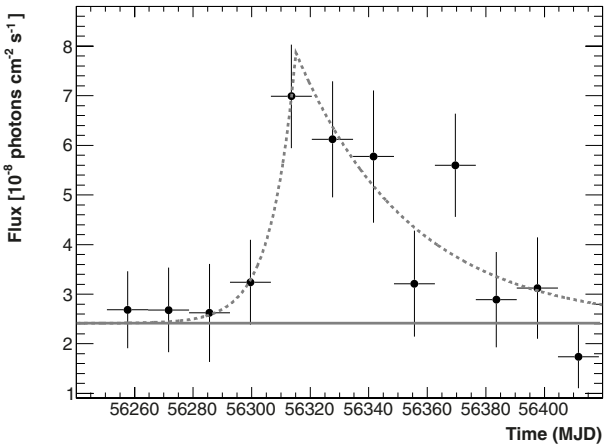

Fig. 5. Flux above 300 MeV of Ap Librae during the flare detected by the *Fermi*-LAT with 14 days integration time. The dashed gray line is the result of the fit with an asymmetric exponential profile (see text) plus a constant (gray line).

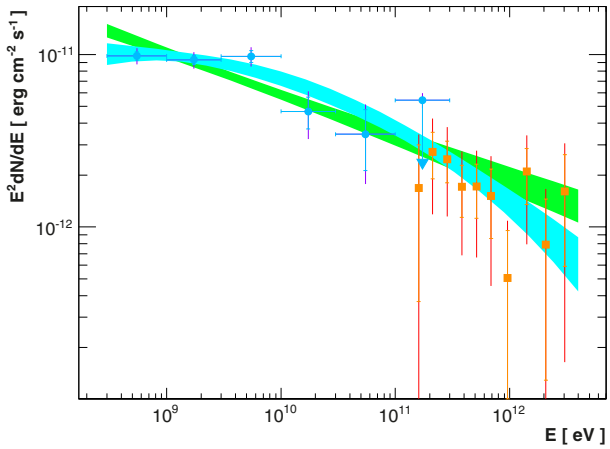

Fig. 6. γ-ray SED of AP Librae from *Fermi*-LAT (blue circles) and H.E.S.S. (orange squares). The green and blue area represent the 68% error contour of the power-law and log-parabola fit to the HE–VHE data.

has the smallest spectral change in the HE–VHE bands, with $\Delta\Gamma = \Gamma_{\rm VHE} - \Gamma_{\rm HE} \sim 0.56 \pm 0.19_{\rm stat} \pm 0.21_{\rm sys}$. We note however that according to the current classification of extragalactic VHE γ-ray emitters in the TeVCaT, (following the classification in the 2LAC), AP Librae would currently be the only VHE γ-ray emitter of the LBL class.

With $\Gamma_{\rm HE} = 2.11$, AP Librae has a rather soft HE spectrum among the population of 2FGL AGN also emitting in the VHE regime, for which the average photon index is $\langle\Gamma_{\rm HE}\rangle = 1.86 \pm 0.26$ (Sanchez et al. 2013). Only the BL Lac object 1RXS J101015.9-311909, BL Lacertae, W Comae and S5 0716+714 exhibit a spectral index $\Gamma_{\rm HE} \geq 2$ (Nolan et al. 2012). The observed peak high energy emission $E_{\rm peak}$ in the SED of objects with $\Gamma_{\rm HE} < 2$ is localized roughly above 10 GeV. This quantity, generally not known before the advent of *Fermi*, is of paramount importance for emission modeling (Tavecchio et al. 1998). We note that, Abramowski et al. (2012) reanalyzed the *Fermi* data of 1RXS J101015.9-311909 above 1 GeV and found a hard index of 1.71, which constrained $E_{\rm peak}$ to be around 100 GeV.

In the next subsection, the peak of the γ-ray emission of Ap Librae is quantified jointly using the data from H.E.S.S. and *Fermi*-LAT.

3.3. Broadband gamma-ray emission of AP Librae

To further investigate the HE–VHE spectral feature, the *Fermi*-LAT best fit power-law spectrum was extrapolated to energies greater than 100 GeV and corrected for the extragalactic background light (EBL) attenuation using the model of Franceschini et al. (2008). A χ^2 comparison of this extrapolation with the H.E.S.S. spectrum yields a χ^2/d.o.f. = 49/10 (probability $P(\chi^2) < 10^{-6}$). The H.E.S.S. systematic uncertainties were included by shifting the energy by 10%[7], which yields an uncertainty of $\sigma(\mathrm{d}N/\mathrm{d}E)_{\rm sys} = 0.1\Gamma_{\rm VHE} \cdot \mathrm{d}N/\mathrm{d}E$ (see Fig. 4). The same comparison based on an extrapolation of the log-parabola spectral hypothesis yields a χ^2/d.o.f. = 8.6/10 (i.e. $P(\chi^2) = 57\%$), which suggests broad band curvature.

To quantify this curvature, the HE and VHE data points (not corrected for EBL) were fitted with power-law and log-parabola models, taking into account the statistical and systematic uncertainties (Fig. 6). In practice, the fit has been done in log-log space with either a first order (power-law) or a second order (log-parabola) polynomial function. The parameters obtained are given in Table 1. The fit of the data with the power-law yields a χ^2/d.o.f. of 26.6/13 (probability of $P(\chi^2) \approx 1\%$), while the log-parabola yields a χ^2/d.o.f. of 7.9/12 (probability of $P(\chi^2) \approx 79\%$). A likelihood ratio test prefers the latter model at a level of 4.3σ, which confirms the presence of curvature in the measured HE–VHE spectrum of AP Librae. However, the fitting method used for the broadband HE–VHE data points differs from the methods used within each energy range and has some limitations (i.e., not taking into account correlations between energy bins). A proper method to overcome such limitations would consist of a joint fit of the data, exploiting the response functions of both space-borne and ground-based γ-ray instruments, which is beyond the scope of this paper.

Correcting the VHE data points for EBL attenuation and repeating the same joint fit, the log-parabola model is then preferred at 2.9σ. In this case the power-law yields a χ^2/d.o.f. of 19.4/13 (probability of $P(\chi^2) \approx 11\%$) and the log-parabola a χ^2/d.o.f. of 9.8/12 (probability of $P(\chi^2) \approx 63\%$). Scaling up the EBL absorption by thirty percent, as in Abramowski et al. (2013), or using the model of Finke et al. (2010) does not significantly affect the latter results because of the rather small redshift of the source.

The EBL attenuation is unlikely to be the only explanation of the spectral break observed in the data. An intrinsic spectral turnover could be due to factors such as a break in the underlying electron energy distribution, the onset of the Klein-Nishina regime in the inverse-Compton emission process, or the absorption of γ rays on the circumnuclear radiation fields (see the discussion on the possibly related phenomenon of GeV breaks observed in the spectra of flat-spectrum radio quasars: e.g., Finke et al. 2008; Ackermann et al. 2010; Tanaka et al. 2011; Aleksić et al. 2011). To elucidate this conundrum would require extensive multi-wavelength modeling of the SED of this complex object[8], which is beyond the scope of this Research Note.

[7] This value is slightly more conservative than the one derived by Meyer et al. (2010) using HE and VHE Crab Nebula data.

[8] See, e.g., Tavecchio et al. (2010) who noted the modeling difficulties with simple synchrotron self-Compton radiative scenarios already when VHE measurements were not yet available and with a shorter *Fermi*-LAT exposure than presented here.

Table 1. Parameters of the first and second degree polynomial functions fit to the HE and VHE data.

Model	p_0	p_1	p_2	χ^2/d.o.f.
Power-law	$-11.48 \pm 0.03_{\rm stat} \pm 0.02_{\rm sys}$	$-2.25 \pm 0.02_{\rm stat} \pm 0.03_{\rm sys}$	–	26.6/13
Log-parabola	$-11.43 \pm 0.04_{\rm stat} \pm 0.03_{\rm sys}$	$2.37 \pm 0.04_{\rm stat} \pm 0.03_{\rm sys}$	$-0.08 \pm 0.02_{\rm stat} \pm 0.01_{\rm sys}$	7.9/12

Notes. The functions are of the form $f(x) = \log_{10}(\mathrm{d}N/\mathrm{d}E) = p_0 + p_1 x$ and $f(x) = \log_{10}(\mathrm{d}N/\mathrm{d}E) = p_0 + p_1 x + p_2 x^2$ with $x \equiv \log_{10}(E/100\ \mathrm{GeV})$.

The description of the HE–VHE emission of AP Librae by a log-parabola allows $E_{\rm peak}$ of AP Librae to be estimated at $10^{2.65 \pm 0.93_{\rm stat} \pm 0.45_{\rm sys}}$ MeV. This value of about 450 MeV is compatible with the low-energy boundary of the *Fermi*-LAT range and could then be considered as an upper limit. It can be compared to the values of $E_{\rm peak}$ determined by Abdo et al. (2010c, d) for the objects BL Lacertae, W Comae and S5 0716+714, using jointly Fermi and publicly available VHE spectra (30 MeV, 4100 MeV, and 800 MeV, respectively). Such low-energy emission peaks are rather uncommon with respect to the bulk of extragalactic VHE emitters, which tend to have maximum emissions at or above hundreds of GeV. The broadband emission of AP Librae is also rather peculiar, as discussed by Fortin et al. (2010) and Kaufmann et al. (2013), with an SED dominated by inverse-Compton and an X-ray spectrum that cannot be explained by synchrotron emission, and that might originate from the same mechanism as the γ-ray emission. This is consistent with a high-energy component shifted toward lower energies and a peak location that could be below the *Fermi*-LAT energy range.

4. Conclusions

The LBL class of VHE emitting objects proves to be an interesting laboratory to test radiative model scenarios, and perhaps to identify parameters on which the LBL–HBL sequence could depend. At present, only a handful of LBL objects have been detected at VHE (or just this one, depending on the selection criteria), probably as a result of a bias toward HBL objects in observation strategies and because LSP objects are the smallest subset of all γ-ray selected BL Lac objects (Shaw et al. 2013). Observations with the H.E.S.S. II telescope, and the advent of the Cherenkov Telescope Array (CTA), which will open the possibility to perform an extragalactic survey (20% of the sky in 100 h) with a sensitivity approaching one percent of the flux of the Crab Nebula (Dubus et al. 2012), should allow more LBL-type blazars to be detected, and give better insights into the physical processes at work.

Acknowledgements. The support of the Namibian authorities and of the University of Namibia in facilitating the construction and operation of H.E.S.S. is gratefully acknowledged, as is the support by the German Ministry for Education and Research (BMBF), the Max Planck Society, the French Ministry for Research, the CNRS-IN2P3 and the Astroparticle Interdisciplinary Programme of the CNRS, the UK. Particle Physics and Astronomy Research Council (PPARC), the IPNP of the Charles University, the South African Department of Science and Technology and National Research Foundation, and by the University of Namibia. We appreciate the excellent work of the technical support staff in Berlin, Durham, Hamburg, Heidelberg, Palaiseau, Paris, Saclay, and in Namibia in the construction and operation of the equipment. The *Fermi* LAT Collaboration acknowledges support from a number of agencies and institutes for both development and the operation of the LAT as well as scientific data analysis. These include NASA and DOE in the United States, CEA/Irfu and IN2P3/CNRS in France, ASI and INFN in Italy, MEXT, KEK, and JAXA in Japan, and the K. A. Wallenberg Foundation, the Swedish Research Council and the National Space Board in Sweden. Additional support from INAF in Italy and CNES in France for science analysis during the operations phase is also gratefully acknowledged. The authors want to acknowledge the anonymous referee for his/her help that greatly improved the paper.

References

Abdo, A. A., Ackermann, M., Ajello, M., et al. 2009a, ApJS, 183, 46
Abdo, A. A., Ackermann, M., Ajello, M., et al. 2009b, ApJ, 700, 597
Abdo, A. A., Ackermann, M., Ajello, M., et al. 2009c, ApJ, 707, 1310
Abdo, A. A., Ackermann, M., Ajello, M., et al. 2010a, ApJ, 710, 810
Abdo, A. A., Ackermann, M., Ajello, M., et al. 2010b, ApJ, 715, 429
Abdo, A. A., Ackermann, M., Agudo, I., et al. 2010c, ApJ, 716, 30
Abdo, A. A., Ackermann, M., Ajello, M., et al. 2010d, ApJ, 722, 520
Abramowski, A., Acero, F., Aharonian, F., et al. 2012, ApJ, 746, 151
Abramowski, A., Acero, F., Aharonian, F., et al. 2013, A&A, 550, A4
Ackermann, M., Ajello, M., Baldini, L., et al. 2010, ApJ, 721, 1383
Ackermann, M., Ajello, M., Allafort, A., et al. 2011, ApJ, 743, 171
Ackermann, M., Ajello, M., Albert, A., et al. 2012, ApJS, 203, 4
Aharonian, F., Akhperjanian, A. G., Bazer-Bachi, A. R., et al. 2006, A&A, 457, 899
Aharonian, F., Akhperjanian, A. G., Bazer-Bachi, A. R., et al. 2007, ApJ, 664, L71
Albert, J., Aliu, E., Anderhub, H., et al. 2007, ApJ, 666, L17
Aleksić, J., Antonelli, L. A., Antoranz, P., et al. 2011, ApJ, 730, L8
Anderhub, H., Antonelli, L. A., Antoranz, P., et al. 2009, ApJ, 704, L129
Armstrong, P., Chadwick, P. M., Cottle, P. J., et al. 1999, Exp. Astron., 9, 51
Atwood, W. B., Abdo, A. A., Ackermann, M., et al. 2009, ApJ, 697, 1071
Berge, D., Funk, S., & Hinton, J. 2007, A&A, 466, 1219
Biraud, F. 1971, Nature, 232, 178
Bolton, J. G., Gardner, F. F., & Mackey, M. B. 1964, Aust. J. Phys., 17, 340
Bond, H. E. 1971, ApJ, 167, L79
Chadwick, P. M., Lyons, K., McComb, T. J. L., et al. 1999, ApJ, 521, 547
Cutini, S. 2011, ATel, 3368, 1
Cutini, S. 2012, ATel, 4028, 1
de Naurois, M. & Rolland, L. 2009, Astropart. Phys., 32, 231
Disney, M. J., Peterson, B. A., & Rodgers, A. W. 1974, ApJ, 194, L79
Dubus, G., Contreras, J. L., Funk, S., et al. 2013, Astropart. Phys., 43, 317
Feldman, G. J., & Cousins, R. D. 1998, Phys. Rev. D, 57, 3873
Finke, J. D., Dermer, C. D., & Böttcher, M. 2008, ApJ, 686, 181
Finke, J. D., Razzaque, S., & Dermer, C. D. 2010, ApJ, 712, 238
Fortin, P., Fegan, S., Horan, D., et al. 2010, in 25th Texas Symp. Relativistic Astrophysics, Proc. Science PoS(Texas2010), 199
Fossati, G., Maraschi, L., Celotti, A., Comastri, A., & Ghisellini, G. 1998, MNRAS, 299, 433
Franceschini, A., Rodighiero, G., & Vaccari, M. 2008, A&A, 487, 837
Hartman, R. C., Bertsch, D. L., Bloom, S. D., et al. 1999, ApJS, 123, 79
H.E.S.S. Collaboration, Abramowski, A., Acero, F., et al. 2012, A&A, 542, A94
Hofmann, W. 2010, ATel, 2743, 1
Johnston, K. J., Fey, A. L., Zacharias, N., et al. 1995, AJ, 110, 880
Jones, D. H., Read, M. A., Saunders, W., et al. 2009, MNRAS, 399, 683
Kaufmann, S., Wagner, S. J., & Tibolla, O. 2013, ApJ, 776, 68
Kaufmann, S., Wagner, S., & Tibolla, O. 2011, Proc. 32nd Int. Cos. Ray Conf. (ICRC2011), 8, 201
Li, T.-P., & Ma, Y.-Q. 1983, ApJ, 272, 317
Mattox, J. R., Bertsch, D. L., Chiang, J., et al. 1996, ApJ, 461, 396
Meyer, M., Horns, D., & Zechlin, H.-S. 2010, A&A, 523, A2
Nolan, P. L., Abdo, A. A., Ackermann, M., et al. 2012, ApJS, 199, 31
Padovani, P., & Giommi, P. 1995, ApJ, 444, 567
Piron, F., Djannati-Atai, A., Punch, M., et al. 2001, A&A, 374, 895
Saito, S., Stawarz, Ł., Tanaka, Y. T., et al. 2013, ApJ, 766, L11
Sanchez, D. A., Fegan, S., & Giebels, B. 2013, A&A, 554, A75
Schwartz, D. A., & Ku, W. H.-M. 1983, ApJ, 266, 459
Shaw, M. S., Romani, R. W., Cotter, G., et al. 2013, ApJ, 764, 135
Sokolovsky, K. V., Schinzel, F. K., & Wallace, E. 2010, ATel, 2402, 1
Strittmatter, P. A., Serkowski, K., Carswell, R., et al. 1972, ApJ, 175, L7
Tanaka, Y. T., Stawarz, Ł., Thompson, D. J., et al. 2011, ApJ, 733, 19
Tavecchio, F., Maraschi, L., & Ghisellini, G. 1998, ApJ, 509, 608

Tavecchio, F., Ghisellini, G., Ghirlanda, G., Foschini, L., & Maraschi, L. 2010, MNRAS, 401, 1570
Vaughan, S., Edelson, R., Warwick, R. S., & Uttley, P. 2003, MNRAS, 345, 1271
Woo, J.-H., Urry, C. M., van der Marel, R. P., Lira, P., & Maza, J. 2005, ApJ, 631, 762
Zhang, Y. H., Celotti, A., Treves, A., et al. 1999, ApJ, 527, 719

[1] Universität Hamburg, Institut für Experimentalphysik, Luruper Chaussee 149, 22761 Hamburg, Germany
[2] Max-Planck-Institut für Kernphysik, PO Box 103980, 69029 Heidelberg, Germany
[3] Dublin Institute for Advanced Studies, 31 Fitzwilliam Place, 2 Dublin, Ireland
[4] National Academy of Sciences of the Republic of Armenia, Yerevan, Armenia
[5] Yerevan Physics Institute, 2 Alikhanian Brothers St., 375036 Yerevan, Armenia
[6] Institut für Physik, Humboldt-Universität zu Berlin, Newtonstr. 15, 12489 Berlin, Germany
[7] Universität Erlangen-Nürnberg, Physikalisches Institut, Erwin-Rommel-Str. 1, 91058 Erlangen, Germany
[8] University of Namibia, Department of Physics, 13301 Private Bag, Windhoek, Namibia
[9] University of Durham, Department of Physics, South Road, Durham DH1 3LE, UK
[10] DESY, 15738 Zeuthen, Germany
[11] Institut für Physik und Astronomie, Universität Potsdam, Karl-Liebknecht-Strasse 24/25, 14476 Potsdam, Germany
[12] Nicolaus Copernicus Astronomical Center, ul. Bartycka 18, 00-716 Warsaw, Poland
[13] Department of Physics and Electrical Engineering, Linnaeus University, 351 95 Växjö, Sweden
[14] Institut für Theoretische Physik, Lehrstuhl IV: Weltraum und Astrophysik, Ruhr-Universität Bochum, 44780 Bochum, Germany
[15] Institut für Astro- und Teilchenphysik, Leopold-Franzens-Universität Innsbruck, 6020 Innsbruck, Austria
[16] Laboratoire Leprince-Ringuet, École Polytechnique, CNRS/IN2P3, 91128 Palaiseau, France
[17] Now at Santa Cruz Institute for Particle Physics, Department of Physics, University of California at Santa Cruz, Santa Cruz, CA 95064, USA
[18] Centre for Space Research, North-West University, 2520 Potchefstroom, South Africa
[19] LUTH, Observatoire de Paris, CNRS, Université Paris Diderot, 5 place Jules Janssen, 92190 Meudon, France
[20] LPNHE, Université Pierre et Marie Curie Paris 6, Université Denis Diderot Paris 7, CNRS/IN2P3, 4 place Jussieu, 75252, Paris Cedex 5, France
[21] Institut für Astronomie und Astrophysik, Universität Tübingen, Sand 1, 72076 Tübingen, Germany
[22] DSM/Irfu, CEA Saclay, 91191 Gif-Sur-Yvette Cedex, France
[23] Astronomical Observatory, The University of Warsaw, Al. Ujazdowskie 4, 00-478 Warsaw, Poland
[24] School of Physics, University of the Witwatersrand, 1 Jan Smuts Avenue, Braamfontein, 2050 Johannesburg, South Africa
[25] Landessternwarte, Universität Heidelberg, Königstuhl, 69117 Heidelberg, Germany
[26] Oskar Klein Centre, Department of Physics, Stockholm University, Albanova University Center, 10691 Stockholm, Sweden
[27] Wallenberg Academy Fellow
[28] Université Bordeaux 1, CNRS/IN2P3, Centre d'Études Nucléaires de Bordeaux Gradignan, 33175 Gradignan, France
[29] Funded by contract ERC-StG-259391 from the European Community,
[30] School of Chemistry & Physics, University of Adelaide, 5005 Adelaide, Australia
[31] APC, AstroParticule et Cosmologie, Université Paris Diderot, CNRS/IN2P3, CEA/Irfu, Observatoire de Paris, Sorbonne Paris Cité, 10 rue Alice Domon et Léonie Duquet, 75205 Paris Cedex 13, France,
[32] UJF-Grenoble 1/CNRS-INSU, Institut de Planétologie et d'Astrophysique de Grenoble (IPAG) UMR 5274, 38041 Grenoble, France
[33] Department of Physics and Astronomy, The University of Leicester, University Road, Leicester, LE1 7RH, UK
[34] Instytut Fizyki Jądrowej PAN, ul. Radzikowskiego 152, 31-342 Kraków, Poland
[35] Laboratoire Univers et Particules de Montpellier, Université Montpellier 2, CNRS/IN2P3, CC 72, Place Eugène Bataillon, 34095 Montpellier Cedex 5, France
[36] Laboratoire d'Annecy-le-Vieux de Physique des Particules, Université de Savoie, CNRS/IN2P3, 74941 Annecy-le-Vieux, France
[37] Obserwatorium Astronomiczne, Uniwersytet Jagielloński, ul. Orla 171, 30-244 Kraków, Poland
[38] Toruń Centre for Astronomy, Nicolaus Copernicus University, ul. Gagarina 11, 87-100 Toruń, Poland
[39] Department of Physics, University of the Free State, PO Box 339, 9300 Bloemfontein, South Africa,
[40] Charles University, Faculty of Mathematics and Physics, Institute of Particle and Nuclear Physics, V Holešovičkách 2, 180 00 Prague 8, Czech Republic
[41] US Naval Research Laboratory, Code 7653, 4555 Overlook Ave. SW, Washington, DC 20375-5352, USA
[42] Fred Lawrence Whipple Observatory, Harvard-Smithsonian Center for Astrophysics, Amado, AZ 85645, USA